New signature of dark matter annihilations: Gamma rays from intermediate-mass black holes

Gianfranco Bertone,[1] Andrew R. Zentner,[2] and Joseph Silk[3]

[1]*Particle Astrophysics Center, Fermi National Accelerator Laboratory, Batavia, Illinois 60510-0500, USA*
[2]*Kavli Institute for Cosmological Physics and Department of Astronomy and Astrophysics, The University of Chicago, Chicago, Illinois 60637, USA*
[3]*Astrophysics, Denys Wilkinson Building, Keble Road, Oxford OX1 3RH, United Kingdom*

(Received 21 September 2005; published 16 November 2005)

We study the prospects for detecting gamma rays from dark matter (DM) annihilations in enhancements of the DM density (mini-spikes) around intermediate-mass black holes (IMBH) with masses in the range $10^2 \lesssim M/\mathrm{M}_\odot \lesssim 10^6$. Focusing on two different IMBH formation scenarios, we show that, for typical values of mass and cross section of common DM candidates, mini-spikes, produced by the adiabatic growth of DM around pregalactic IMBHs, would be bright sources of gamma rays, which could be easily detected with large field-of-view gamma-ray experiments such as GLAST, and further studied with smaller field-of-view, larger-area experiments like Air Cherenkov Telescopes CANGAROO, HESS, MAGIC, and VERITAS. The detection of many gamma-ray sources not associated with a luminous component of the Local Group, and with identical cutoffs in their energy spectra at the mass of the DM particle, would provide a potential smoking-gun signature of DM annihilations and shed new light on the nature of intermediate and supermassive black holes.

DOI: 10.1103/PhysRevD.72.103517 PACS numbers: 95.35.+d, 97.60.Lf, 98.62.Js, 98.70.Sa

I. INTRODUCTION

Although many astrophysical and cosmological observations provide convincing evidence for the existence of a ''dark'' component in the matter density of the Universe, the nature of this *dark matter* (DM) remains unknown. It is commonly assumed that DM is made of new, as yet undiscovered, particles, associated with theories beyond the standard model of particle physics. Among the most widely studied candidates are the supersymmetric neutralino and candidates arising in theories with extra dimensions, which appear difficult to constrain with direct searches (i.e. by looking for nuclear recoils due to DM particles scattering off nuclei) and whose prospects of discovery at future accelerators strongly depend on the details of the particle physics setup (for recent reviews see e.g. Refs. [1,2]). Indirect searches via the detection of annihilation radiation may provide an interesting alternative, but they are usually affected by large astrophysical and cosmological uncertainties. Furthermore, in many cases, the detection of an annihilation signal may be difficult to distinguish from less exotic astrophysical sources. An example of this is the case of the galactic center, where such high-energy radiation has been recently observed by several different experiments, without providing any conclusive evidence for or against an interpretation in terms of DM annihilation products (see Refs. [3–7] and references therein).

Here we describe a scenario that may provide smoking-gun evidence for the annihilation of DM particles. If intermediate-mass black holes (IMBHs), with a mass ranging between 10^2 and 10^6 $\mathrm{M}_\odot$ (e.g. [8]), exist in the Galaxy, their adiabatic growth would have modified the DM distribution around them, leading to the formation of ''mini-spikes,'' that is, large, local enhancements of the DM density [9]. The DM annihilation rate being proportional to the square of the number density of DM particles, these mini-spikes would be bright gamma-ray sources, distributed in a roughly spherically symmetric way about the galactic center, and well within the observational reach of the next-generation gamma-ray experiments. Their brightness and isotropy make them ideal targets of large field-of-view gamma-ray experiments such as GLAST [10]. In case of a positive detection, Air Cherenkov Telescopes such as CANGAROO [11], HESS [12], MAGIC [13], and VERITAS [14] could extend the observations to higher energies and improve the angular resolution. We argue that the observation of numerous (up to $\sim$100) pointlike gamma-ray sources with identical cutoffs in their energy spectra, at an energy equal to the mass of the DM particle, would provide smoking-gun evidence for DM particles.

In this paper, we make predictions for the number of detectable black holes in two different IMBH formation scenarios. In the first scenario, IMBHs form in rare, overdense regions at high redshift, $z \sim 20$, as remnants of Population III stars, and have a characteristic mass scale of a few 10^2 $\mathrm{M}_\odot$ [15] (a similar scenario was investigated in Ref. [9,16,17]). In this scenario, these black holes serve as the seeds for the growth supermassive black holes found in galactic spheroids [18]. In the second scenario, IMBHs form directly out of cold gas in early forming halos, in a sense that will be specified below, and are typified by a larger mass scale, of order 10^5 $\mathrm{M}_\odot$. We demonstrate that, with respect to Ref. [9], the latter scenario leads to qualitative differences in the mini-spike profiles with dramatic consequences for the detectability of gamma-ray fluxes. For both scenarios, we make detailed estimates of the

population of IMBH in the Milky Way (MW) DM halo using a complete model of IMBH formation at high redshift, black hole mergers, and halo merger and evolution [19]. This allows us the unique ability to make a detailed study of the detectabilty of mini-spikes as gamma-ray sources.

This paper is organized as follows. In Sec. II A, we review the evidence and formation scenarios for IMBHs. In Sec. II B, we describe the model that we employ to estimate the properties of the local IMBH population, and we present the main properties (radial profile, mass function, etc.) of IMBH populations in Milky Way-like halos in Sec. II C. Section III is devoted to the calculation of the mini-spike profiles and Sec. IV to the DM annihilation fluxes. Section V contains our primary results on the observability of gamma rays from the annihilation of DM around IMBHs. In Sec. VI, we discuss the implications of our results and draw our conclusions. We perform all of our calculations in the context of a standard, flat cosmological constant plus cold DM (ΛCDM) cosmology with $\Omega_{\rm M} = 0.3$, $\Omega_\Lambda = 0.7$, $h = 0.7$ and a scale-invariant primordial power spectrum with a normalization set by $\sigma_8 = 0.9$.

II. EVIDENCE AND PROPERTIES OF IMBHS

A. The case for IMBHs

In the last few years, observational and theoretical evidence has accumulated [8] for the existence of compact objects, heavier than *stellar* black holes, but lighter than the so-called *supermassive* black holes (SMBHs) lying at the centers of galactic spheroids. We consider here the mass range $20 \lesssim M_{\rm IMBH}/{\rm M}_\odot \lesssim 10^6$, where the lower bound of the IMBHs mass corresponds to recent estimates of the maximum mass of the remnant of a massive stellar collapse [20], and the upper limit roughly indicates the minimum mass of SMBHs, assumed to lie in the range $10^6 \lesssim M_{\rm SMBH}/{\rm M}_\odot \lesssim 10^9$ (see e.g. Ref. [18] for a recent review).

A hint of the existence of IMBHs is provided by the detection of bright, x-ray, point sources, called ultraluminous x-ray sources (ULXs), that are apparently not associated with active galactic nuclei [21–23]. Although many known x-ray sources are associated with neutron stars and black holes, this interpretation fails in the case of ULXs. ULXs would have to emit radiation far above the Eddington limit, if $M \lesssim 20\ {\rm M}_\odot$, and their positions in their host galaxies are not compatible with masses $M \gtrsim 10^6\ {\rm M}_\odot$, because dynamical friction would cause these objects to sink to the centers of their hosts on a time scale shorter than a Hubble time (e.g. Ref. [8]). Accretion by IMBHs has been advocated as a possible explanation [17]. Another hint for the existence of IMBHs, although not conclusive, comes from stellar kinematics in globular clusters [24]; the observed relation between the mass and the velocity dispersion in selected globular clusters may fall on the extrapolation of the analogous relation for SMBHs [25–27].

From a theoretical point of view, a population of massive seed black holes could help to explain the origin of SMBHs. In fact, observations of quasars at redshift $z \approx 6$ in the Sloan digital survey [28–30] suggest that SMBHs were already in place when the Universe was only $\sim$1 Gyr old, a circumstance that can be understood in terms of rapid growth starting from massive seeds (see e.g. Ref. [31]). Furthermore, the growth of SMBHs through accretion and merging of heavy seeds may aid in the understanding of some of the observed relationships between supermassive black hole masses and the properties of their host galaxies and halos [32–37]. Scenarios that seek to explain the properties of the observed supermassive black hole population generally result in the prediction of a concomitant population of ''wandering'' IMBHs throughout massive DM halos and the intergalactic medium [19,38,39]. However, despite their theoretical interest, it is difficult to obtain conclusive evidence for the existence of IMBHs. A viable detection strategy could be the search for gravitational waves produced in the mergers of the IMBH population [19,40–44], which may become possible with the advent of space-based interferometers such as LISA.

B. IMBHs formation scenarios

We focus here on two scenarios leading to the formation of black holes at very different mass scales. In the first scenario (which we refer to as *scenario A*), black holes are remnants of the collapse of Population III (or ''first'') stars [15]. Numerical simulations suggest that the first stars may form when primordial molecular clouds with $\approx 10^5\ {\rm M}_\odot$ cool by formation and destruction of H_2 into cold pockets at the centers of their DM halos, with typical densities of order $10^4\ {\rm cm}^{-3}$ and temperatures of order a few $\times\ 10^2$ K [45,46], and become gravitationally unstable.

Newtonian simulations suggest that the fate of Pop III stars is very different from the case of their metal-enriched, comparably less massive counterparts mentioned above. Zero metallicity Pop III stars with masses in the range $M \sim$ 60-140 $\rm M_\odot$ and $M \gtrsim 260\ {\rm M}_\odot$ collapse directly to black holes, stars with $140 \lesssim M/{\rm M}_\odot \lesssim 260\ {\rm M}_\odot$ are completely disrupted due to the pulsation-pair-production instability, leaving behind no remnant, and again stars with masses $M \gtrsim 260\ {\rm M}_\odot$ collapse directly to black holes [47] (see also Refs. [48–51]). The evolution time scale of these very massive stars is typically of order $t_* \sim$ 1-10 Myr. After this time scale, supernovae begin to explode, releasing energy and metals into the surrounding medium. In the standard picture of hierarchical structure formation, the metal-enriched material will be collected at later times at the centers of more massive halos, where new generations of stars will form.

Interestingly, if a $\sim 10^2\ {\rm M}_\odot$ black hole forms halos that represent $\sim 3\sigma$ peaks of the smoothed density field, the

resulting baryonic mass fraction in these objects would be comparable with the mass fraction in SMBHs [15]. Additionally, such a scenario leads to the natural prediction of a population of wandering black holes in the halos of Milky Way-sized galaxies, with masses similar to their initial mass scale $M \sim 10^2$ $M_\odot$, as many of the relatively small halos ($M \sim 10^7$ $M_\odot$ for 3σ fluctuations at $z = 18$) that host early forming black holes do not merge with the central galaxy, but orbit about the periphery of the halo [19,38,39]. We stress that black holes in this scenario may not necessarily form at the very centers of their initial host dark matter halos at high redshift, a circumstance that, as we shall see, may have important consequences on the detectability of IMBHs.

To represent the predictions of this class of black hole formation scenario where black holes form at $\sim$100 $M_\odot$ from the remnants of the first stars, we use a model similar to that proposed by Madau and Rees [15] and studied in further detail by Islam *et al.* [38] and Volonteri *et al.* [39]. Specifically, at $z = 18$, we populate halos that constitute 3σ peaks in the smoothed primordial density field with seed black holes of initial mass 100 $M_\odot$. We evolve these halos using an analytic model of halo growth that is focused on making many statistical realizations of the growth of a Milky Way-sized halo. After populating progenitor halos at high redshift with black holes as described above, these processes of halo growth and evolution are treated as described in detail in [19,52–54]. We refer the reader to these references for details and tests of the halo evolution models. For the purposes of this study, we take the mass of the Milky Way halo to be $M_{\rm MW} = 10^{12.1}\ h^{-1}$ $M_\odot$ and perform 200 statistical realizations in order to ascertain the expected range of observable IMBHs.

The second scenario that we consider (*scenario B*) is based on the proposal of Ref. [37] and it is representative of a class of models in which black holes originate from massive objects formed directly during the collapse of primordial gas in early forming halos [55–60]. In this class of models, the initial black holes are massive ($\sim 10^5$ $M_\odot$) and the growth of SMBH proceeds in such a way that both mergers and accretion play an important role. We use the model of Ref. [37] to represent the predictions of models that start SMBH growth from very massive seeds. The proposal of Ref. [37] is as follows. During the virialization and collapse of the first halos, gas cools, collapses, and forms pressure-supported disks at the centers of halos that are sufficiently massive to contain a relatively large amount of molecular hydrogen (molecular hydrogen is the primary gas coolant in halos in the relevant mass range, see [61] for a review). In halos that are both massive enough that molecular hydrogen cooling is efficient and which do not experience any major mergers over a dynamical time, a protogalactic disk forms and can evolve uninterrupted. An effective viscosity due to local gravitational instabilities in the disk leads to an effective viscosity that transfers mass inward and angular momentum outward [62] until supernovae in the first generation of stars heat the disk and terminate this process [37]. By the time the process terminates (of order the lifetimes of Pop III stars, $\sim$1-10 Myr), a baryonic mass of order $\sim 10^5$ $M_\odot$ loses its angular momentum and is transferred to the center of the halo. Such an object may be briefly pressure supported, but it eventually collapses to form a black hole [47,63].

The requirements that the early forming host halo be massive enough to form an unstable disk and that the halo not experience a major merger imprints a typical mass scale for halos within which this process occurs of order $\sim 10^7$ $M_\odot$. In this case the characteristic mass of the black hole forming in a halo of virial mass M_v is given by

$$M_{\rm bh} = 3.8 \times 10^4\ M_\odot \left(\frac{\kappa}{0.5}\right)\left(\frac{f}{0.03}\right)^{3/2}\left(\frac{M_v}{10^7 M_\odot}\right)\left(\frac{1+z}{18}\right)^{3/2} \times \left(\frac{t}{10\ {\rm Myr}}\right), \quad (1)$$

where we have assumed that a fraction f is the fraction of the total baryonic mass in the halo that has fallen into the disk, z is the redshift of formation, κ is that fraction of the baryonic mass which loses its angular momentum that remains in the remnant black hole, and t is the time scale for the evolution of the first generation of stars [37]. The distribution of black hole masses is a log-normal distribution with a mean given by the characteristic mass above and a standard deviation $\sigma_{M_{\rm bh}} = 0.9$. The spread is determined by the spread in total angular momentum exhibited by halos of fixed mass in cosmological N-body simulations of DM halo formation [64]. Using the prescriptions of the Koushiappas *et al.* [37] model, we can again populate halos with black holes at high redshift and evolve them forward to determine the properties of satellite black holes in a statistically large sample of Milky Way-like halos at $z = 0$. This is precisely what was done in Ref. [19] in order to study the gravity wave background and we refer the reader to this work for further details. As with scenario A, we take the Milky Way halo to have mass $M_{\rm MW} = 10^{12.1}\ h^{-1}$ $M_\odot$ at $z = 0$ and construct 200 realizations of wandering black hole populations in halos of this mass.

C. Intermediate-Mass Black Holes in Milky Way-sized Halos

In the previous two sections, we outlined models for the production of IMBHs in the early universe and evolution of IMBHs in their host halos in the context of the hierarchical cold dark matter (CDM) model of structure formation. Of course, as halos merge to form larger systems that eventually grow to the size of the Milky Way, black holes merge, producing supermassive, central black holes and perhaps a detectable gravity wave signal. These products have been the focus of most previous work regarding these models [19,37,39,65]. Consequently, these studies focused much attention on the merging of black holes as halos and

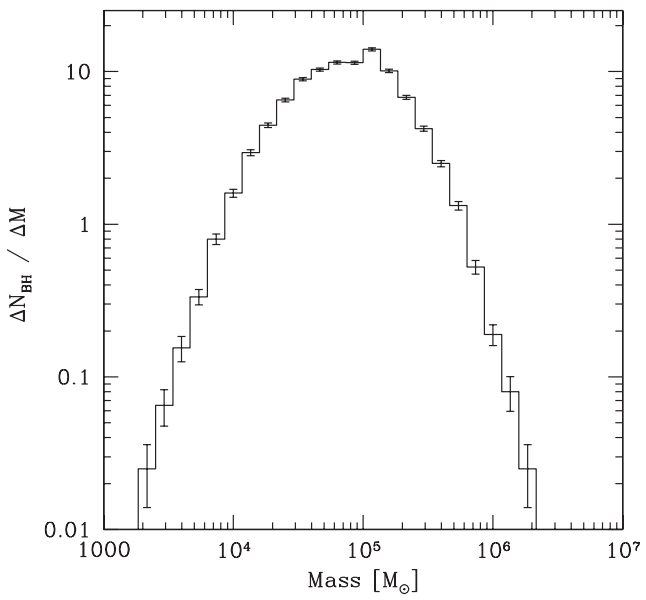

FIG. 1. Mass function of unmerged IMBHs in the scenario B, for a Milky Way halo at $z = 0$. The distribution is based on an average of 200 Monte Carlo realizations of a halo of virial mass $M_v = 10^{12.1}\ h^{-1}\ M_\odot$, roughly the size of the halo of the Milky Way.

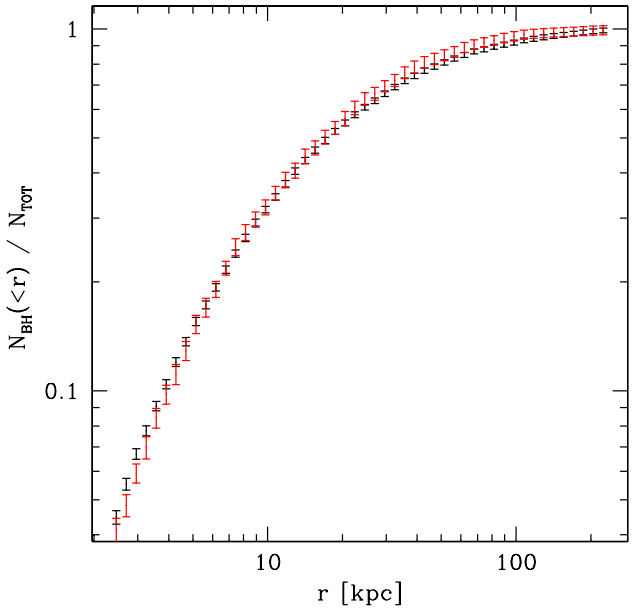

FIG. 2 (color online). Cumulative radial distribution of unmerged IMBHs in the scenario A (gray) and B (black), for a Milky Way halo at $z = 0$. The mean and error are based on 200 Monte Carlo realizations of IMBH populations in Milky Way-sized halos. Notice that unlike subhalo populations, IMBHs do not exhibit a significant antibias with respect to the DM. Rather, they are slightly biased toward being found near the halo center.

galaxies merge. On the contrary, we are most interested in those pristine black holes that are orbiting within the Milky Way halo and have not merged with other black holes because these unmerged black holes may still reflect the properties of the dark matter density enhancement in which they formed.

In scenario A, the mass spectrum of unmerged black holes is a delta function as described in Section II A. The average number of *unmerged* black holes per Milky Way halo is $N_{\rm bh,A} \simeq 1027 \pm 84$, where the error bar denotes the 1σ scatter from halo to halo. In scenario B, the total number of *unmerged* black holes per Milky Way halo is $N_{\rm bh,B} \simeq 101 \pm 22$. We show in Fig. 1 the final mass spectrum (i.e. at redshift $z = 0$) of black holes in scenario B. As expected the distribution follows closely the initial mass spectrum, with a characteristic mass of order $\approx 10^5\ M_\odot$. The only deviation is that the overall distribution is slightly broadened by the fact that not all black holes form at the same redshift in halos of the same mass (see Eq. (1) and Refs. [19,37]). The radial distribution of unmerged black holes is less trivial, and it would be more difficult to derive directly from the models of IMBH formation at high redshift. The distribution is essentially set by the energy and angular momentum distributions of merging objects in a ΛCDM cosmology and dynamical friction (e.g. [53]). Unlike dark matter substructures, which are generally absent from the inner parts of the host halos, because they tend to lose mass via tidal mass loss and heating, black holes and the surrounding dark matter distribution in the vicinity of the IMBHs can survive tidal disruption to very small galactocentric distances. The final, cumulative radial distributions of unmerged IMBHs are shown in Fig. 2. They are very similar for scenarios A and B (though the normalization is different), and shows a behavior that scales as $dN/dr \sim r^{-3}$ at large scales and tends toward a shallower slope on scales smaller than the scale radii of typical MW-size halos (see the following section).

III. THE DENSITY ENHANCEMENT OF DARK MATTER AROUND IMBHS

In each early forming halo that hosts a seed black hole, when the black hole forms the DM distribution about the black hole inevitably reacts, adjusting to the new gravitational potential. This process has been studied extensively, particularly in the context of stellar cusps around massive black holes in clusters of stars or at the centers of galaxies (see e.g. [66–69]). Gondolo and Silk have applied this argument to the distribution of DM at the center of the Galaxy [70] and introduced the term "spike" for the consequent enhancement in the DM density around the central SMBH, in order to avoid confusion with DM "cusps" at the centers of halos in the *cold* dark matter model of structure formation. It was subsequently shown that dynamical processes like off-center formation of the seed black hole, or major merger events, may lead to destruction or reduction of the spike [71,72]. However, steeply rising

stellar cusps in the innermost regions of galaxies suggest that such processes were not effective, at least in the case of the Milky Way, or that the stellar cusps were regenerated via star formation [73] or energy exchange between stars [74].

Recently, Bertone and Merritt studied the evolution of DM spikes including gravitational scattering off stars and the self-annihilation of DM particles [6,7], showing that the DM density in spikes is, indeed, substantially reduced by these effects, but the enhancement of the annihilation signal is still significant with respect to ordinary DM cusps.

In the present study, we are interested in ''mini-spikes'' surrounding IMBHs. Because we track the merger history of each individual black hole, we can select precisely those black holes which never experienced mergers, to ensure that major mergers have not destroyed any cusp that existed around the original black hole.

Furthermore, the models we explore predict from between a few hundred to a few thousand black holes scattered throughout the Milky Way halo, and as the Milky Way has only 11 luminous companions within $\sim$300 kpc [75], we expect that the majority of the wandering black holes in our models reside in satellite halos with no significant stellar component.

This implies that the effects of scattering off of stars should not significantly alter the DM distributions around the wandering IMBHs. The mini-spikes around unmerged, wandering, IMBHs are thus less sensitive to all of the dynamical processes that may have affected the spike at the galactic center.

We proceed now to evaluate the DM enhancements around IMBHs. As a first step, we need to specify the ''initial'' DM profile, that is, the DM distribution prior to black hole formation. Let the subscript ''f'' denote quantities at the time when the IMBH formed. The initial DM profile of the mini-halo, before adiabatic growth, can be well approximated with a Navarro, Frenk, and White (NFW) profile [76]

$$\rho(r) = \rho_0 \left(\frac{r}{r_s}\right)^{-1} \left(1 + \frac{r}{r_s}\right)^{-2}. \tag{2}$$

The normalization constant ρ_0, and the scale radius r_s, can be expressed in terms of the virial mass of the halo at the time when the IMBH formed $M_{\mathrm{vir},f}$, and the virial concentration parameter $c_{\mathrm{vir},f}$

$$r_s = \frac{r_{\mathrm{vir},f}}{c_{\mathrm{vir},f}}, \qquad \rho_0 = \frac{M_{\mathrm{vir},f}}{4\pi r_s^3 f(c_{\mathrm{vir,f}})}. \tag{3}$$

We recall that the virial mass is related to the virial radius $r_{\mathrm{vir},f}$ by

$$M_{\mathrm{vir},f} = \frac{4\pi}{3}[\Delta_{\mathrm{vir}}(z_f)\rho_m(z_f)] r_{\mathrm{vir},f}^3, \tag{4}$$

while the function $f(x)$ is, apart from constants, simply the volume integral of the NFW profile $f(x) \equiv \ln(1+x) - [x/(1+x)]$.

In Eq. (4), $\rho_m(z_f)$ is the mean DM density at the redshift of formation z_f, while $\Delta_{\mathrm{vir}}(z_f)$ is the virial overdensity, for which we have adopted here the fitting form of Bryan and Norman [77]. At the redshifts of interest ($z \gtrsim 12$) the Universe is DM-dominated and the expansion rate and growth of perturbations are described by the standard relations for an $\Omega_{\mathrm{M}} = 1$, ''standard'' CDM cosmology. In this case, $\Delta_{\mathrm{vir}}(z_f) \simeq 18\pi^2 \simeq 178$. For each black hole at redshift $z = 0$ we extract from its merger tree the parameters $M_{\mathrm{vir},f}$, $c_{\mathrm{vir,f}}$, z_f and use Eq. (2) to calculate the initial DM profile before the formation of the black hole. Alternatively, we could have chosen the more recent parametrization proposed by Navarro *et al.* [78] (see also Refs. [79,80]). However, this profile implies modifications at scales smaller than those we are interested in, where the profile is anyway modified by the presence of the IMBH.

We assume that the black holes form over a time scale long enough to guarantee adiabaticity, but short compared to the cosmological evolution of the host halo (in scenario B, both of these assumptions are built into the black hole formation model, see Section II B as well as our discussion below).

Adiabaticity requires that the formation time of the black hole is much larger than the dynamical time scale at a distance r_h from the black hole, where r_h is the radius of the sphere of gravitational influence of the black hole, $r_h \simeq GM_{\mathrm{bh}}/\sigma^2$, and σ is the velocity dispersion of DM particles at r_h. In practice, we estimate r_h by solving the implicit equation

$$M(<r_h) \equiv \int_0^{r_h} \rho(r) r^2 \mathrm{d}r = 2M_{\mathrm{bh}}. \tag{5}$$

For a representative case in scenario B, with $M_{\mathrm{bh}} = 10^8\ \mathrm{M}_\odot$ and $M_{\mathrm{vir},f} = 10^8\ \mathrm{M}_\odot$, this gives $r_h/r_s \approx 0.04$. In scenario B, the black hole formation time is set by the time scale for viscous angular momentum loss and is limited by the evolutionary time scale of the first stars and the gravitational infall time across the gaseous disk, which is of order Myr (see Ref. [19] for a detailed discussion of time scales). The relevant time scale for the mass build up of the IMBH is then $t_{ev} \sim$ 1-20 Myr. In scenario A, we follow Ref. [9] where the characteristic time scale for the growth of the black hole by accretion is taken to be of order 1-20 Myr for a plausible range of accretion efficiencies.

The basics of adiabatic growth can be easily understood (e.g. Ref. [2]), and in most cases the details can be worked out by taking into account the approximate conservation of adiabatic invariants under a certain set of assumptions. If one starts from an initially uniform DM distribution, the final profile will be a mild mini-spike with density $\rho_{\mathrm{sp}} \propto (r/r_h)^{3/2}$ (e.g. see [69] and references therein). If one starts from a cuspy profile, such as the NFW profile of Eq. (2), the new profile is essentially a power law,

$$\rho_{\rm sp}(r) = \rho(r_{\rm sp})\left(\frac{r}{r_{\rm sp}}\right)^{-\gamma_{\rm sp}}, \quad (6)$$

where the radius of the spike is $r_{\rm sp} \approx 0.2 r_h$ [81], and $\gamma_{\rm sp}$ is related to the initial power-law index γ by [70]

$$\gamma_{\rm sp} = \frac{9-2\gamma}{4-\gamma}. \quad (7)$$

In the case of the profile of Eq. (2), this reduces to $\gamma_{\rm sp} = 7/3$.

The DM annihilation flux in this case diverges at small radii. However, the very annihilations that we study here provide an upper limit to the DM number (and thus mass) density. In absence of other processes affecting the distribution of DM, the DM density obeys the equation

$$\dot{n}_\chi(r,t) = -\sigma v\, n_\chi^2(r,t), \quad (8)$$

where σv is the annihilation cross section times relative velocity (in the nonrelativistic limit) and $m\chi$ is the DM particle mass. The solution to the evolution equation is

$$n_\chi(r,t) = \frac{n_\chi(r,t_f)}{1 + n_\chi(r,t_f)\sigma v (t-t_f)} \quad (9)$$

which shows that efficient annihilations set an upper limit to the matter density of order $m_\chi/\sigma v(t-t_f)$. We define $r_{\rm lim}$ as the radius where

$$\rho_{\rm sp}(r_{\rm lim}) = m_\chi/\sigma v(t-t_f) \equiv \rho_{\rm lim}. \quad (10)$$

We therefore define an inner cutoff at a radius

$$r_{\rm cut} = {\rm Max}[4R_{\rm Schw}, r_{\rm lim}], \quad (11)$$

where $R_{\rm Schw}$ is the Schwarzschild radius of the IMBH $R_{\rm Schw} = 2.95\ {\rm km}\ M_{\rm bh}/{\rm M}_\odot$. For common values of the mass and cross section of the DM particle, $r_{\rm lim} \sim 10^{-3}$ pc so that $r_{\rm cut} = r_{\rm lim}$.

Is the adiabatic growth of a central mass a good approximation in our IMBH formation scenarios? We have already discussed the time scales involved, but the derivation of the inner radius $r_{\rm lim}$ provides us with the possibility of checking whether the size of the region where matter accretes, leading to the formation of a black hole, is actually smaller than the characteristic size of the DM spike, $r_{\rm lim}$. In scenario A, this is not a problem, because in this case the black holes from Pop. III stars and the spike is produced by the *growth* of the black hole, thus by processes occurring on scales of order $R_{\rm Schw} \ll r_{\rm lim}$. In scenario B, the situation is different, because the mini-spike is produced by the flow of protogalactic material that lost its angular momentum by viscosity.

Such an object may collapse directly to a black hole or it may form a short-lived, pressure-supported object [47,63]. However, in either case, the characteristic size of the massive object that forms is likely to be much smaller than $r_{\rm lim}$. We can make an order-of-magnitude estimate of the relative sizes as follows. Massive stars are believed to have a polytropic equation of state with $n = 3$. In other words, the equation of state is described by

$$P(r) = K\rho(r)^\Gamma, \qquad \Gamma = 1 + 1/n, \quad (12)$$

and in this case $n = 3$ implies $\Gamma = 4/3$, as appropriate for a star supported by radiation pressure. It is possible to evaluate numerically the properties of a polytropic star in hydrostatic equilibrium, for $n = 3$ the approximate relation $\rho_c = 54.2\bar{\rho}$ between the central and the average density of the star holds (see e.g. [82]).

We infer that the typical scale for the radial extent of such an object should be

$$R_* = \left(54.2\frac{3M_*}{4\pi\rho_c}\right)^{1/3} \approx 10^{-5}\ {\rm pc}\left(\frac{M}{10^5\ {\rm M}_\odot}\right)^{1/3}\left(\frac{\rho_c}{10^{-2}\ {\rm g\ cm^{-3}}}\right)^{-1/3}. \quad (13)$$

This scale is clearly much smaller than the typical size of the spike $r_{\rm cut}$.

IV. DARK MATTER ANNIHILATIONS IN MINI-SPIKES

Dark matter particles are expected to have a non-negligible annihilation cross section into standard model particles, in order to be kept in chemical equilibrium in the early universe. It should be a weak or weaker-than-weak interaction in order to provide a relic density which satisfies cosmological constraints (for recent reviews of DM candidates and detection techniques see e.g. Refs. [1,2]). Although it is difficult to make definitive statements on the nature of the DM particles, it is commonly believed that a mass in the range $m_\chi \sim$ 100-1000 GeV would be a reasonable expectation in the most widely discussed DM scenarios (e.g. minimal supersymmetry or scenarios with unified extra dimensions). A naïve estimate of the annihilation cross section, based on the observed relic abundance of DM, suggests that $\sigma v \sim 10^{-26}\ {\rm cm^3\ s^{-1}}$. This value can be more appropriately used as an upper limit to the annihilation cross section, rather than an actual estimate, since processes like coannihilations may significantly affect relic density yields (for more details see Refs. [1,2] and references therein).

Instead of undertaking a detailed scan of the parameter space for different DM candidates, we limit ourselves here to estimates of the annihilation fluxes for two benchmark models: an optimistic model, with $m_\chi = 100$ GeV and $\sigma v = 3 \times 10^{-26}\ {\rm cm^3\ s^{-1}}$, leading to large annihilation fluxes; and a model with $m_\chi = 1$ TeV and $\sigma v = 10^{-29}\ {\rm cm^3\ s^{-1}}$, leading to more pessimistic predictions. We note that in both cases, the mini-spike profiles reach their maximum values at a radii $r_{\rm lim} \gg 4R_{\rm Schw}$, thus $r_{\rm lim}$ provides an estimate of the size of the region where most of the annihilation radiation originates from. The case of annihilations from the DM spike at the center of the Galaxy has been extensively studied in the literature in

terms of neutrino, gamma-ray, and synchrotron emission [6,7,70,83–86].

The flux of gamma -rays from a mini-spike around an IMBH can be expressed as

$$\Phi(E, D) = \frac{1}{2}\frac{\sigma v}{m_\chi^2}\frac{1}{D^2}\frac{dN}{dE}\int_{r_{cut}}^{r_{sp}} \rho_{sp}^2(r) r^2 dr = \frac{dN}{dE}\frac{\rho_{sp}^2}{4\gamma_{sp}-6}\frac{\sigma v}{m_\chi^2}\frac{r_{sp}^3}{D^2}\left(\frac{r_{cut}}{r_{sp}}\right)^{-2\gamma_{sp}+3}, \quad (14)$$

where we assumed $r_{sp} \gg r_{cut}$. Inserting typical values of DM and spike parameters we get, for the case $\gamma = 1$ ($\gamma_{sp} = 7/3$),

$$\Phi(E, D) = \Phi_0 \frac{dN}{dE}\left(\frac{\sigma v}{10^{-26}\ \mathrm{cm^3/s}}\right)\left(\frac{m_\chi}{100\ \mathrm{GeV}}\right)^{-2} \times \left(\frac{D}{\mathrm{kpc}}\right)^{-2}\left(\frac{\rho(r_{sp})}{10^2\ \mathrm{GeV\ cm^{-3}}}\right)^2\left(\frac{r_{sp}}{\mathrm{pc}}\right)^{14/3} \times \left(\frac{r_{cut}}{10^{-3}\ \mathrm{pc}}\right)^{-5/3}, \quad (15)$$

with $\Phi_0 = 9 \times 10^{-10}\ \mathrm{cm^{-2}\ s^{-1}}$. It is useful here to emphasize the relative luminosities of IMBHs in the MW halo. In particular, consider the case of the relatively more luminous objects of scenario B. Using the fiducial values adopted in Eq. (15), which are typical of scenario B, one can easily verify that *the "luminosity" of a mini-spike* (proportional to the volume integral of ρ_{sp}^2) *is of the order of the gamma-ray luminosity of the entire Milky Way halo*, a circumstance that has dramatic consequences for the prospects of indirect detection, as we describe in the following section.

To estimate the flux, we need now to specify the gamma-ray spectrum per annihilation dN/dE, which depends on the nature of the DM particle. In most scenarios, direct annihilation in two photons is severely suppressed, but a continuum spectrum is expected from the decay of secondary neutral pions.

In Fig. 3 we show the predicted gamma-ray spectra for different annihilation channels. For the $b\bar{b}$ channel we show two different curves, corresponding to different parametrization of the process of quark fragmentation and subsequent decay of neutral pions, for 2 different mass scales of the DM particle. The first (FPS 04) corresponds to the parametrization in Ref. [87], while the second (BSS 03) refers to the spectra presented in Ref. [88]. The differences for different parametrizations and mass scales appear to be small, The third curve (BUB 97) corresponds to an analytic fit for the WW and ZZ channels, as discussed in Ref. [89] , a channel leading to harder spectra with respect to the quark-antiquark channel. These channels often represent the most important annihilation channels for neutralino dark matter. In the case of Kaluza-Klein DM, other channels become important. Following Ref. [4] we show in Fig. 3 the total spectrum obtained by adding the contribution of different channels, weighted with the appropriate branching ratios. It is evident from the figure that in this case the spectrum is harder than the quark or gauge bosons channels, due to contributions from internal bremsstrahlung as well to decays of quarks and tau leptons. Internal bremsstrahlung is a general feature of scenarios where DM particles annihilate into pairs of charged fermions, which produces a sharp edge feature in the spectrum, dropping abruptly at a photon energy equal to the weakly interacting massive particle (WIMP) mass [4,90,91].

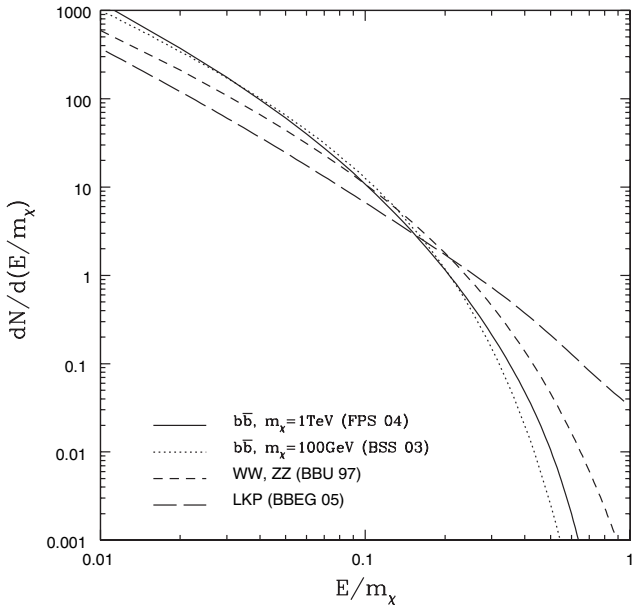

FIG. 3. Energy spectra of photons per annihilation for different annihilation channels. The *solid* and *dotted* lines both correspond to the $b\bar{b}$ annihilation channel, the differences are due to different parametrizations of quark fragmentation and different DM particle mass scales. The *solid* line shows the parametrization of Ref. [87] with $m_\chi = 1$ TeV, while the *dotted* line shows that of Ref. [88] with $m_\chi = 100$ GeV. The *short-dashed* line corresponds to the spectra for annihilation through the WW and ZZ channels. In particular, we show the fit from Ref. [89]. Lastly, the *long-dashed* line shows the spectrum, summed over contributing channels, for annihilation of Kaluza-Klein DM from Ref. [4].

In the next section, we will present our predictions using the BSS 03 spectrum, with the caveat that different annihilation channels may lead to slightly different results. The predictions for different annihilation channels can be easily obtained by plugging the appropriate spectrum per annihilation into Eq. (15).

V. RESULTS

In this section, we present our results on the detectability of annihilation radiation from the density enhancements about IMBHs. The number and properties of the IMBHs population are slightly different from one realization of Milky Way-sized halos to another, as described in Sec. II. To estimate the prospects of detection of IMBHs in the

Milky Way, we thus need to average the results over all realizations.

In Fig. 4, we show the (average) integrated luminosity function of IMBHs in scenario B. We define the integrated luminosity function as the number of black holes producing a gamma-ray flux larger than Φ, as a function of Φ. The upper (lower) line corresponds to $m_\chi = 100$ GeV, $\sigma v = 3 \times 10^{-26}$cm ^{3} s^{-1} ($m_\chi = 1$ TeV, $\sigma v = 10^{-29}$ cm^3 s^{-1}). In a practical sense, the plot shows the number of IMBHs that can be detected with experiments with point-source sensitivity Φ above 1 GeV. We show for comparison the point-source sensitivity above 1 GeV for EGRET and GLAST, corresponding roughly to the flux for a 5σ detection of a high-latitude point source in an observation time of 1 yr [92]. The dashed region corresponds to the 1σ scatter between different realizations of Milky Way-sized halos. This band includes the variation in spatial distributions of IMBHs from one halo to the next as well as the variation in the individual properties of each IMBH in each realization.

Although one would naïvely expect that the fluxes scale with $\sigma v/m_\chi^2$, we note that the DM profile itself depends on m_χ and σv, more precisely on the ratio $\sigma v/m_\chi$ [see Eq. (10)]. The maximum density is higher for the pessimistic case, and this partially compensates for the decrease in flux due to the prefactor $\sigma v/m_\chi^2$. It is easy to see this in the case $\gamma = 1$ from Eq. (15) as, by virtue of Eq. (10), $r_{\rm cut} \propto (\sigma v/m)^{-3/7}$, and the final luminosity of the objects is thus proportional to $\sim(\sigma v)^{2/7} m_\chi^{-9/7}$.

The number of detectable sources is very high, even in the pessimistic case, and either strong constraints on a combination of the astrophysics and particle physics of this scenario, or an actual detection, should be possible within the first year of operation of GLAST, which is expected to be launched in 2007. Depending on the specific scenario, EGRET may have observed some of these IMBH mini-spikes, which would still account only for a small fraction of the unidentified sources.

We show in Fig. 5 the integrated luminosity function of IMBHs in scenario A, for the same particle physics models shown in Fig. 5. The lines and error bars all have the same meaning as those in Fig. 4 for scenario B. In this case of scenario A, mini-spikes are weaker, but the number of black holes is larger by roughly an order of magnitude, so that GLAST may still detect between a few tens and several hundred sources, whereas EGRET may have seen only a few or none.

In Figs. 4 and 5 we have assumed that the main annihilation channel is $b\bar{b}$. Although we have seen in the previous section that, depending on the nature of the DM particle, other channels may dominate and lead to different annihi-

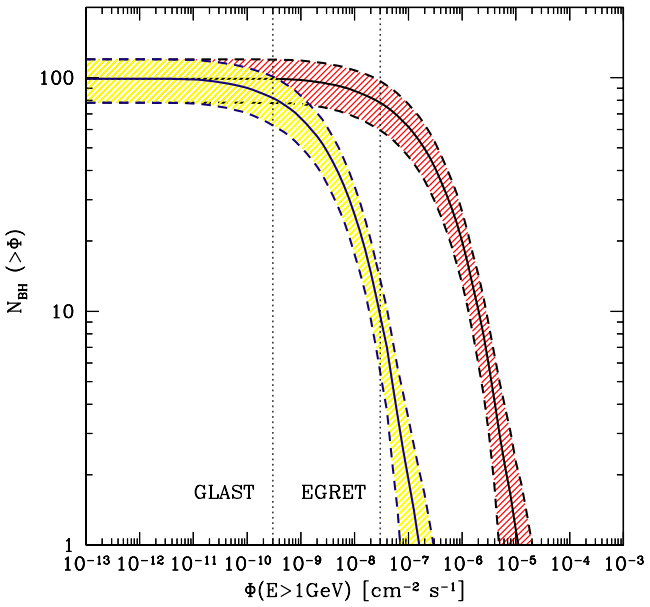

FIG. 4 (color online). IMBHs integrated luminosity function, i.e. number of black holes producing a gamma-ray flux larger than a given flux, as a function of the flux, for our scenario B (i.e. for IMBHs with mass $\sim 10^5$ M$_\odot$). The upper (lower) line corresponds to $m_\chi = 100$ GeV, $\sigma v = 3 \times 10^{-26}$ cm^3 s^{-1} ($m_\chi = 1$ TeV, $\sigma v = 10^{-29}$ cm^3 s^{-1}). For each curve we also show the 1-σ scatter among different realizations of Milky Way-sized host DM halos. The figure can be interpreted as the number of IMBHs that can be detected from experiments with point-source sensitivity Φ (above 1 GeV), as a function of Φ. We show for comparison the 5σ point-source sensitivity above 1 GeV of EGRET and GLAST (1 yr).

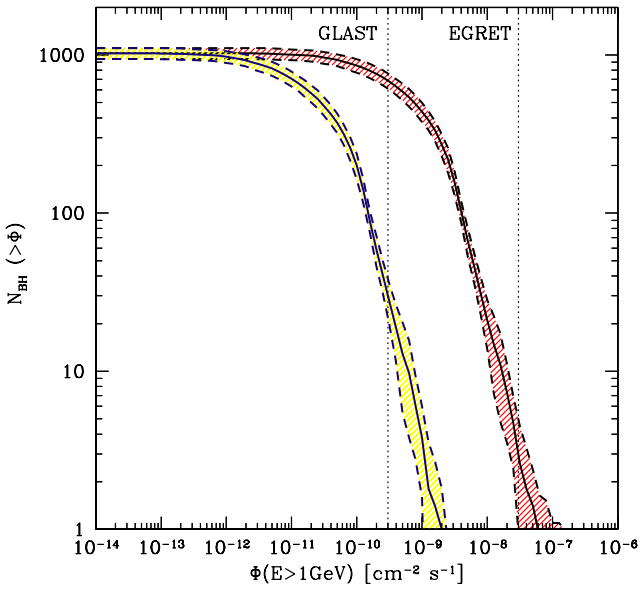

FIG. 5 (color online). IMBHs integrated luminosity function in scenario A (i.e. for IMBHs with mass $\sim 10^2$ M$_\odot$). The upper (lower) line corresponds to $m_\chi = 100$ GeV, $\sigma v = 3 \times 10^{-26}$ cm^3 s^{-1} ($m_\chi = 1$ TeV, $\sigma v = 10^{-29}$ cm^3 s^{-1}). For each curve we also show the 1-σ scatter among realizations of Milky Way-sized halos. For the sake of comparison, we also show the point-source sensitivity above 1 GeV for EGRET and GLAST.

lation spectra. We see from these figures that the expected uncertainty, $\mathcal{O}(1)$, would have a small influence on the number of objects that GLAST should be able to detect, certainly smaller than the uncertainties associated with m_χ and σv and typically smaller than, or comparable to, the 1-σ scatter between different Milky Way halo realizations.

VI. DISCUSSION AND CONCLUSIONS

We have studied the detectability of gamma rays from DM annihilations in mini-spikes around IMBHs. The prospects of detection are summarized in Figs. 4 and 5, where we show the number of IMBHs that can be detected from experiments with point-source sensitivity Φ (above 1 GeV), as a function of Φ. We found that the prospects of detection with GLAST are so promising that a large number of sources may be detected within its first year of operation. With respect to the case of a spike at the galactic center, searching for annihilation radiation from mini-spikes has the obvious disadvantage that IMBHs are smaller than the SMBH at the galactic center, and the mini-spikes grow from less dense initial profiles. However, there are also several advantages.

First of all, it is likely that the vast majority of mini-spikes around *unmerged* IMBHs in the outer galactic halo are not affected by the dynamical processes that tend to destroy the central spike, or to decrease significantly the DM density near the black hole. For instance, they lack stellar cusps and are rarely affected by tidal interactions. Furthermore, the prospects of detectability appear very promising and certainly less problematic than, say, annihilations from the galactic center. In fact, the gamma-ray background is strongest in the direction of the galactic center and substantially reduced when observations are performed off the disk and, in particular, at high galactic latitudes. There is even reason to believe that the number density of IMBH may be *enhanced* at high galactic latitudes [93].

Moreover, there are several known gamma-ray sources in the direction of the galactic center, and the observation of a unique source, even coincident with the Galactic center would not necessarily imply a DM annihilation origin. On the contrary, the detection of tens or more gamma-ray sources with identical spectra, in particular, identical cutoffs at the DM particle mass, and not associated with the galactic disk or other luminous companions of the Milky Way, would provide a smoking-gun signature of DM annihilations.

A natural place to search for IMBHs may be the known dwarf satellite galaxies about the Milky Way; however, the physics that govern the formation of these objects is still a topic of much debate and uncertainty, so such a search may be subject to the same drawbacks as searches for radiation near the center of the Galaxy. However, as we have already stressed, these IMBH formation scenarios have as a virtue that they predict that there may be hundreds of detectable objects within the galactic halo, most of which would not be associated with the known population of dwarf satellite galaxies. An IMBH population similar to the one in the Milky Way halo should be present in Andromeda, given its similarity to the Galaxy in terms of size and mass. Moreover, the distance to the Andromeda IMBHs would be between $\approx$ 400-1000 kpc, amounting to a factor of only a few more in distance than to the black holes of the outer MW halo. Hence the detection of such IMBHs in Andromeda may be possible in optimistic scenarios and may serve to demonstrate the ubiquity of such phenomena.

As a further implication, we found that the annihilation luminosity from any Milky Way-like halo may be dominated by annihilation around IMBHs in optimistic scenarios. As an example, we showed that in scenario B, the total luminosity of an individual mini-spike, in terms of annihilation radiation, may be comparable to the luminosity of the entire host halo. Therefore, such optimistic scenarios provide a significant "boost factor" for the gamma-ray background due to DM annihilations in halos at all redshifts (e.g., Ref. [94], see also Ref. [95] for a comparison between the prospects of indirect detection from the galactic center and the gamma-ray background), as well as an enhancement of antimatter fluxes. A detailed study of these alternative indirect searches requires a full analysis of the redshift evolution of IMBHs and spikes in halos of all masses in the former case, and of the propagation of antiparticles in the Galaxy in the latter, and it is thus beyond the scope of this paper.

Interestingly, the prospects of indirect detection in this scenario do not depend strongly on the particle physics parameters. In fact, while e.g. in the case of annihilations from the galactic center the annihilation flux is proportional to $\sigma v/m_\chi^2$, the flux from mini-spikes is limited by the plateau in the number density due to DM annihilation itself. For mini-spikes growing from $\gamma = 1$ profiles, we have shown that the annihilation flux is instead proportional to $(\sigma v)^{2/7} m_\chi^{-9/7}$.

Finally, we stress that the detection of these sources would shed new light on the origin of IMBHs and SMBHs. Mini-spikes appear to be ideal targets for large field-of-view experiments such as GLAST. Another promising experiment with a large field-of-view could be the Alpha Magnetic Spectrometer (AMS-02) instrument, if preliminary estimates of its sensitivity to gamma rays are confirmed [96]. Once the positions of the sources are determined, Air Cherenkov Telescopes such as CANGAROO [11], HESS [12], MAGIC [13], and VERITAS [14] may provide additional information, because of their better performance at higher energies and significantly better angular resolution. The determination of a common cutoff in the spectra (possible only with ACTs for DM particles heavier than 300 GeV) will provide an estimate of the mass of the DM particle, while spectral features, such as annihilation lines or sharp edges, may

provide important information on the nature of the DM particle.

ACKNOWLEDGMENTS

We would like to thank John Beacom, Pierre Brun, Dan Hooper, Stelios Kazantzidis, Savvas Koushiappas, David Merritt, and Louis Strigari for many helpful discussions. G. B. is supported by the DOE and NASA Grant No. NAG 5-10842 at Fermilab. A. R. Z. is supported by the Kavli Institute for Cosmological Physics at The University of Chicago and by the National Science Foundation under Grant No. NSF PHY 0114422.

[1] L. Bergstrom, Rep. Prog. Phys. **63**, 793 (2000).
[2] G. Bertone, D. Hooper, and J. Silk, Phys. Rep. **405**, 279 (2005).
[3] F. A. Aharonian *et al.*, Astron. Astrophys. **425**, L13 (2004).
[4] L. Bergstrom, T. Bringmann, M. Eriksson, and M. Gustafsson, Phys. Rev. Lett. **94**, 131301 (2005).
[5] D. Hooper and J. March-Russell, Phys. Lett. B **608**, 17 (2005).
[6] G. Bertone and D. Merritt, astro-ph/0501555.
[7] G. Bertone and D. Merritt, Mod. Phys. Lett. A **20**, 1021 (2005).
[8] M. C. Miller and E. J. M. Colbert, Int. J. Mod. Phys. D **13**, 1 (2004).
[9] H. S. Zhao and J. Silk, astro-ph/0501625.
[10] http://www-glast.stanford.edu/
[11] http://icrhp9.icrr.u-tokyo.ac.jp/index.html
[12] http://www.mpi-hd.mpg.de/hfm/HESS/HESS.html
[13] http://hegra1.mppmu.mpg.de/MAGICWeb/
[14] http://veritas.sao.arizona.edu/index.html
[15] P. Madau and M. J. Rees, Astrophys. J. Lett. **551**, L27 (2001).
[16] R. Islam, J. Taylor, and J. Silk, Mon. Not. R. Astron. Soc. **354**, 443 (2004).
[17] R. Islam, J. Taylor, and J. Silk, Mon. Not. R. Astron. Soc. **354**, 427 (2004).
[18] L. Ferrarese and H. Ford, Space Sci. Rev. **116**, 523 (2005).
[19] S. M. Koushiappas and A. R. Zentner, astro-ph/0503511.
[20] C. L. Fryer and V. Kalogera, Astrophys. J. **554**, 548 (2001).
[21] E. Colbert and A. Ptak, Astrophys. J. Suppl. Ser. **143**, 25 (2002).
[22] D. A. Swartz, K. K. Ghosh, A. F. Tennant, and K. Wu, astro-ph/0405498.
[23] G. C. Dewangan, R. E. Griffiths, M. Choudhury, T. Miyaji, and N. J. Schurch, astro-ph/0508431.
[24] J. Frank and M. J. Rees, Mon. Not. R. Astron. Soc. **176**, 633 (1976).
[25] K. Gebhardt, R. M. Rich, and L. C. Ho, Astrophys. J. Lett. **578**, L41 (2002).
[26] R. P. van der Marel, J. Gerssen, P. Guhathakurta, R. C. Peterson, and K. Gebhardt, Astron. J. **124**, 3255 (2002).
[27] J. Gerssen, R. P. van der Marel, K. Gebhardt, P. Guhathakurta, R. C. Peterson, and C. Pryor, Astron. J. **124**, 3270 (2002).
[28] X. Fan *et al.* (SDSS Collaboration), Astron. J. **122**, 2833 (2001).
[29] A. J. Barth, P. Martini, C. H. Nelson, and L. C. Ho, Astrophys. Lett. **594**, L95 (2003).
[30] C. J. Willott, R. J. McLure, and M. J. Jarvis, Astrophys. J. **587**, L15 (2003).
[31] Z. Haiman and A. Loeb, Astrophys. J. **552**, 459 (2001).
[32] J. Kormendy and D. Richstone, Annu. Rev. Astron. Astrophys. **33**, 581 (1995).
[33] L. Ferrarese and D. Merritt, Astrophys. J. **539**, L9 (2000).
[34] R. J. McLure and J. S. Dunlop, Mon. Not. R. Astron. Soc. **331**, 795 (2002).
[35] K. Gebhardt *et al.*, Astrophys. J. **539**, L13 (2000).
[36] S. Tremaine *et al.*, Astrophys. J. **574**, 740 (2002).
[37] S. M. Koushiappas, J. S. Bullock, and A. Dekel, Mon. Not. R. Astron. Soc. **354**, 292 (2004).
[38] R. Islam, J. Taylor, and J. Silk, Mon. Not. R. Astron. Soc. **340**, 647 (2003).
[39] M. Volonteri, F. Haardt, and P. Madau, Astrophys. J. **582**, 559 (2003).
[40] K. S. Thorne and V. B. Braginskii, Astrophys. J. Lett. **204**, L1 (1976).
[41] É. É. Flanagan and S. A. Hughes, Phys. Rev. D **57**, 4566 (1998).
[42] É. É. Flanagan and S. A. Hughes, Phys. Rev. D **57**, 4535 (1998).
[43] R. Islam, J. Taylor, and J. Silk, Mon. Not. R. Astron. Soc. **354**, 629 (2004).
[44] T. Matsubayashi, H. Shinkai, and T. Ebisuzaki, Astrophys. J. **614**, 864 (2004).
[45] T. Abel, G. L. Bryan, and M. L. Norman, Astron. Astrophys. **540**, 39 (2000).
[46] V. Bromm, P. S. Coppi, and R. B. Larson, Astrophys. J. **564**, 23 (2002).
[47] A. Heger, C. L. Fryer, S. E. Woosley, N. Langer, and D. H. Hartmann, Astrophys. J. **591**, 288 (2003).
[48] J. R. Bond, W. D. Arnett, and B. J. Carr, Astrophys. J. **280**, 825 (1984).
[49] C. L. Fryer, S. E. Woosley, and A. Heger, Astrophys. J. **550**, 372 (2001).
[50] R. B. Larson, astro-ph/9912539.
[51] R. Schneider, A. Ferrara, B. Ciardi, V. Ferrari, and S. Matarrese, Mon. Not. R. Astron. Soc. **317**, 385 (2000).
[52] A. R. Zentner and J. S. Bullock, Astrophys. J. **598**, 49 (2003).
[53] A. R. Zentner, A. A. Berlind, J. S. Bullock, A. V. Kravtsov, and R. H. Wechsler, Astrophys. J. **624**, 505 (2005).
[54] S. M. Koushiappas, A. R. Zentner, and T. P. Walker, Phys. Rev. D **69**, 043501 (2004).
[55] M. G. Haehnelt and M. J. Rees, Mon. Not. R. Astron. Soc. **263**, 168 (1993).

[56] A. Loeb and F. A. Rasio, Astrophys. J. **432**, 52 (1994).
[57] D. J. Eisenstein and A. Loeb, Astrophys. J. **443**, 11 (1995).
[58] M. G. Haehnelt, P. Natarajan, and M. J. Rees, Mon. Not. R. Astron. Soc. **300**, 817 (1998).
[59] O. Y. Gnedin, Classical Quantum Gravity **18**, 3983 (2001).
[60] V. Bromm and A. Loeb, Astrophys. J. **596**, 34 (2003).
[61] M. Tegmark, J. Silk, M. J. Rees, A. Blanchard, T. Abel, and F. Palla, Astrophys. J. **474**, 1 (1997).
[62] D. N. C. Lin and J. E. Pringle, Mon. Not. R. Astron. Soc. **225**, 607 (1987).
[63] S. L. Shapiro and S. A. Teukolsky, *Black Holes, White Dwarfs, and Neutron Stars* (Wiley-Interscience, New York, 1983).
[64] J. S. Bullock, A. Dekel, T. S. Kolatt, A. V. Kravtsov, A. A. Klypin, C. Porciani, and J. R. Primack, Astrophys. J. **555**, 240 (2001).
[65] A. Sesana, F. Haardt, P. Madau, and M. Volonteri, Astrophys. J. **611**, 623 (2004).
[66] P. J. E. Peebles, Astrophys. J. **178**, 371 (1972).
[67] P. Young, Astrophys. J. **242**, 1232 (1980).
[68] J. R. Ipser and P. Sikivie, Phys. Rev. D **35**, 3695 (1987).
[69] G. D. Quinlan, L. Hernquist, and S. Sigurdsson, Astrophys. J. **440**, 554 (1995).
[70] P. Gondolo and J. Silk, Phys. Rev. Lett. **83**, 1719 (1999).
[71] P. Ullio, H. Zhao, and M. Kamionkowski, Phys. Rev. D **64**, 043504 (2001).
[72] D. Merritt, M. Milosavljevic, L. Verde, and R. Jimenez, Phys. Rev. Lett. **88**, 191301 (2002).
[73] M. Milosavljevic and A. Loeb, Astrophys. J. **604**, L45 (2004).
[74] M. Preto, D. Merritt, and R. Spurzem, Astrophys. J. **613**, L109 (2004).
[75] M. Mateo, Annu. Rev. Astron. Astrophys. **36**, 435 (1998).
[76] J. F. Navarro, C. S. Frenk, and S. D. M. White, Astrophys. J. **490**, 493 (1997).
[77] G. L. Bryan and M. L. Norman, Astrophys. J. **495**, 80 (1998).
[78] J. F. Navarro *et al.*, Mon. Not. R. Astron. Soc. **349**, 1039 (2004).
[79] D. Reed, F. Governato, L. Verde, J. Gardner, T. Quinn, J. Stadel, D. Merritt, and G. Lake, Mon. Not. R. Astron. Soc. **357**, 82 (2005).
[80] D. Merritt, J. Navarro, A. Ludlow, and A. Jenkins, Astrophys. J. **624**, L85 (2005).
[81] D. Merritt, astro-ph/0301257.
[82] S. Chandrasekhar *An Introduction to the Study of Stellar Structure* (Dover, New York, 1967).
[83] P. Gondolo, Phys. Lett. B **494**, 181 (2000).
[84] G. Bertone, G. Sigl, and J. Silk, Mon. Not. R. Astron. Soc. **326**, 799 (2001).
[85] G. Bertone, G. Sigl, and J. Silk, Mon. Not. R. Astron. Soc. **337**, 98 (2002).
[86] R. Aloisio, P. Blasi, and A. V. Olinto, J. Cosmol. Astropart. Phys. 05 (2004) 007.
[87] N. Fornengo, L. Pieri and S. Scopel, Phys. Rev. D **70**, 103529 (2004).
[88] G. Bertone, G. Servant, and G. Sigl, Phys. Rev. D **68**, 044008 (2003).
[89] L. Bergstrom, P. Ullio, and J. H. Buckley, Astropart. Phys. **9**, 137 (1998).
[90] J. F. Beacom, N. F. Bell, and G. Bertone, Phys. Rev. Lett. **94**, 171301 (2005).
[91] A. Birkedal, K. T. Matchev, M. Perelstein, and A. Spray, hep-ph/0507194.
[92] A. Morselli, A. Lionetto, A. Cesarini, F. Fucito, and P. Ullio (GLAST Collaboration), Nucl. Phys. B, Proc. Suppl. **113**, 213 (2002).
[93] A. R. Zentner, A. V. Kravtsov, O. Y. Gnedin, and A. A. Klypin, Astrophys. J. **629**, 219 (2005).
[94] P. Ullio, L. Bergström, J, Edsjö, and C. Lacey, Phys. Rev. D **66**, 123502 (2002).
[95] S. Ando, Phys. Rev. Lett. **94**, 171303 (2005).
[96] P. Brun, L. Girard, and S. Rosier-Lees, in preparation.